Supplement Table

	Metabolite Tissue Content micromole/gdw				Metabolic Flux Data		
	Glutamate	Alpha - Ketoglutarate	Citrate	Aspartate	Acetyl CoA Enrichment from Palmitate	Citric Acid Cycle Flux	Rate of palmitate oxidation
dbdb	7.39 ± 0.59	0.23 ± 0.02	0.51 ±0.09	2.68 ±0.37	0.70 ± 0.02	16.00 ± 2.27	1.39 ± 0.17
dbdb ISC/REP	8.27 ± 0.91	0.25 ± 0.02	0.51 ± 0.05	2.59 ± 0.17	0.76 ± 0.03	9.99 ±0.41	0.95 ±0.05
c57bl/6	9.42 ± 0.70	0.23 ±0.02	0.47 ± 0.03	2.43 ± 0.19	0.68 0.02	13.41 ±1.48	1.14 ± 0.12
c57bl/6 ISC/REP	9.38 ± 1.25	0.28 0.02	0.51 ± 0.06	2.55 ± 0.21	0.76 ± 0.03	12.14 ± 0.14	1.2 ± 0.04

Supplemental Table Tissue metabolite content and flux data used for modeling kinetic flux. Data is representative of the averages for the groups. It is important to note that kinetic flux measurements and M/A shuttle activity was modeled for each individual experiment, not from averages. C57bl/6: N = 6; c57bl/6 + ISC/REP: N = 6; db/db: N = 6; db/db + ISC/REP: N = 7.

Supplemental Figure 1

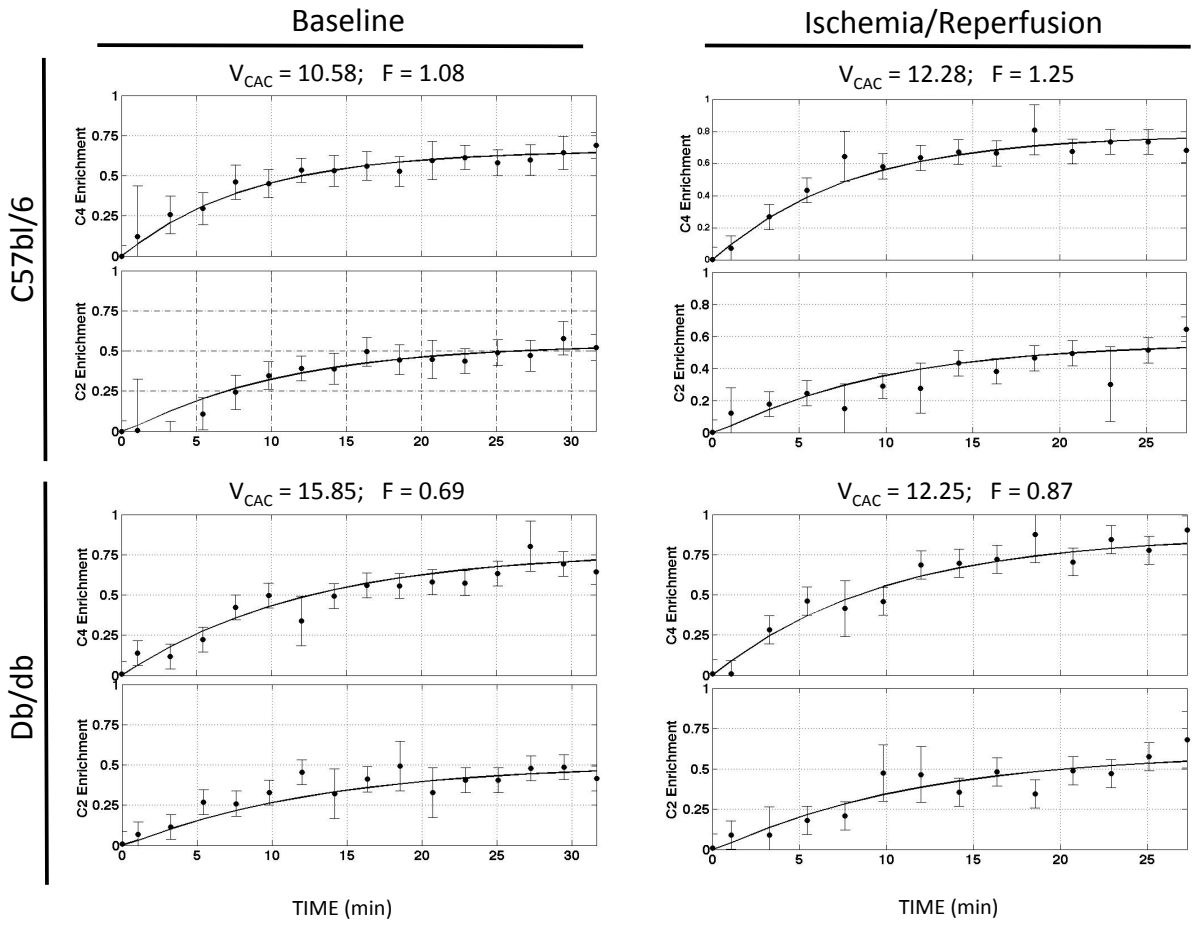

Supplemental Figure 1 Representative C4/C2 enrichment curves from kinetic modeling from four individual experiments. Enrichment curves above represent findividual experiments, and do not reflect the averaged metabolite data from Supplemental Table 1. Accordingly, each experiment above is from an experiment with different rate pressure products and metabolite contents, which will influence the flux parameters for the consistence of the kinetics of enrichment and input data. The curves represent a “goodness of fit” of experimental enrichment and metabolite data.

Supplemental Methods

NMR spectroscopy and tissue chemistry. Measurements of TAG turnover were performed on intact beating hearts that were situated within a 10 mm broad band NMR probe inside a 14.1 T NMR magnet. Sequential, proton-decoupled ^{13}C NMR spectra were acquired (2 min each) with natural ^{13}C abundance correction using previously reported NMR methods [1-3]. Magnetic field homogeneity was optimized by shimming to a proton line width of 10-20 Hz.

Carbon-13 enrichment of TAG in the intact heart was monitored from the NMR signal at 30.5 ppm from the TAG methylene groups and TAG turnover was calculated from total TAG content and enrichment over time [4-6]. Kinetic analysis of dynamic ^{13}C-spectra from intact, beating hearts was performed as previously reported from our laboratory [1, 2, 4, 6]. Carbon spectra were acquired at 100 MHz, with bilevel broad-band decoupling and subtracted from naturally abundant endogenous ^{13}C signal.

Tissue metabolites were extracted from frozen heart tissue using 7% perchloric acid and neutralized with KOH. Tissue extracts were analyzed spectrophotometrically and flurometically for quantificaiton [7, 8]. Glutamate concentration was determined with glutamate dehydrogenase and diaphorase (Roche L-Glutamic acid colorimetric kit.) α-Ketoglutarate content was measured by coupling glutamate-oxaloacetate transaminate (GOT, Roche) with malate dehydrogenase (MDH, Roche) in the presence of excess L-aspartate. Aspartate concentration was measured by coupling GOT with MDH similar to α-ketoglutarate with the exception of excess α-ketoglutarate. Citrate content was determined with citrate lyase (Roche) and MDH. *In vitro* high-resolution ^{13}C NMR spectra of tissue extracts reconstituted in 0.5 mL of D_2O were collected with a 5 mm ^{13}C probe (Bruker Instruments, Billerica, MA). Analysis was performed to determine fractional enrichment of [2-^{13}C] acetyl CoA [9, 10].

Kinetic Analysis Oxidative Rates. A set of nine differential equations describes the concentration history of the ^{13}C in each metabolite and developed in our laboratory was modified to include the additional, rate-determining components of long chain fatty acid uptake into the mitochondria. With a single 9x1 vector q to represent the fractional enrichment of each compartment as a function of time, the model is described in matrix form as

$$\frac{d}{dt}q = M_{TCA} \cdot q + U_{Acetyl-CoA}$$

where M_{TCA} is a 9x9 matrix characteristic of the TCA cycle, its elements are determined by the TCA cycle flux (V_{TCA}), the interconversion rates between the TCA cycle intermediate and glutamate or aspartate (F_1 and F_2), the level of anaplerosis (y), and the concentrations of each metabolite. The input vector, $U_{Acetyl\text{-}CoA}$, is governed by the fraction of ^{13}C enriched acetyl-CoAentering the TCA cycle through citrate synthase (F_c). The only non-zero element in $U_{Acetyl\text{-}CoA}$ corresponds to the labeling of the 4-carbon position of citrate since [2-^{13}C] acetyl-CoA enters the TCA cycle through citrate synthase to enrich the 4-carbon position of citrate [4, 11, 12]. The nine differential equation in series are:

$$\frac{d}{dt}CIT4 = \frac{V_{TCA}}{[CIT]} \cdot (F_c - CIT4)$$

$$\frac{d}{dt}\alpha KG4 = \frac{V_{TCA}}{[\alpha KG]} \cdot CIT4 - \frac{V_{TCA} + F_1}{[\alpha KG]} \cdot \alpha KG4 + \frac{F_1}{[\alpha KG]} \cdot GLU4$$

$$\frac{d}{dt}GLU4 = \frac{F_1}{[GLU]} \cdot (\alpha KG4 - GLU4)$$

$$\frac{d}{dt}CIT2 = \frac{V_{TCA}}{[CIT]} \cdot (OAA2 - CIT2)$$

$$\frac{d}{dt}\alpha KG2 = \frac{V_{TCA}}{[\alpha KG]} \cdot CIT2 - \frac{V_{TCA} + F_1}{[\alpha KG]} \cdot \alpha KG2 + \frac{F_1}{[\alpha KG]} \cdot GLU2$$

$$\frac{d}{dt}GLU2 = \frac{F_1}{[GLU]} \cdot (\alpha KG2 - GLU2)$$

$$\frac{d}{dt}MAL2 = \frac{V_{TCA}}{[MAL]} \cdot [\frac{1}{2} \cdot \alpha KG2 + \frac{1}{2} \cdot \alpha KG4 - (1 + y) \cdot MAL2]$$

$$\frac{d}{dt}OAA2 = \frac{V_{TCA}}{[OAA]} \cdot MAL2 - \frac{V_{TCA} + F_2}{[OAA]} \cdot OAA2 + \frac{F_2}{[OAA]} \cdot ASP2$$

$$\frac{d}{dt}ASP2 = \frac{F_2}{[ASP]} \cdot (OAA2 - ASP2)$$

Where CIT, aKG, GLU, MAL, OAA, and ASP denote the metabolites citrate, a-ketoglutarate, glutamate, malate, oxaloacetate, and aspartate, respectively, with the corresponding number of the ^{13}C enriched carbon position indicated. Where CIT4 is the fractional enrichment level of ^{13}C at the 4-carbon position of citrate; (i.e., CIT4=[(4-^{13}C)CIT]/[CIT]). The equation describing malate enrichment includes anaplerotic and cataplerotic effects [1, 9, 12]. F_1 and F_2 are fluxes for interconversion via both transamination and membrane transport, between a-ketoglutarate and glutamate, and between aspartate and oxaloacetate, respectively. Under the current experimental conditions of limited aspartate and alanine, $F_1 = F_2$ [1, 9, 11, 12].

A penalty function was applied, using MVO_2 as an external measured parameter, to constrain optimization of fitting data to the kinetic model within the known physiological limits [9, 12]:

$$\tilde{f}(\mathbf{p}) = \sum_{i=1}^{m} \left(\frac{d(t_i, \mathbf{p}) - s(t_i)}{\sigma_i} \right)^2 + \left(\frac{V_{TCA} - V_{MVO_2}}{\sigma_{MVO_2}} \right)^2$$

Where t_i are the data-sampling times, $d(t_i,p)$ are glutamate enrichment predicted by the model, $s(t_i)$ are the NMR measurements of glutamate enrichment, and σ_i are the error associate with NMR measurements. V_{TCA} and V_{MVO2} are measured from oxygen consumption rate and σ_{MVO2} is the error associate with the measurement of oxygen consumption [9, 12].

The rate of palmitate oxidation (R) was calculated, under these precise experimental and isotopic enrichment conditions, as the product of V_{TCA} and acetyl CoA enrichment from ^{13}C palmitate (F_c) divided by 8 to account for the 8 acetyl groups produced from the 16 carbon palmitate (V_{TCA} x F_c/8).

Statistical Analysis Inter-group statistics were analyzed using one-way ANOVA analysis with the Tukey post-test. Statistical significance was established at 5% probability ($P < 0.05$). All reported values are reported as averages ± SEM.

References:

[1] O'Donnell JM, Alpert NM, White LT, Lewandowski ED. Coupling of mitochondrial fatty acid uptake to oxidative flux in the intact heart. Biophys J. 2002;82:11-8.
[2] O'Donnell JM, Zampino M, Alpert NM, Fasano MJ, Geenen DL, Lewandowski ED. Accelerated triacylglycerol turnover kinetics in hearts of diabetic rats include evidence for compartmented lipid storage. American journal of physiology Endocrinology and metabolism. 2006;290:E448-55.
[3] Banke NH, Wende AR, Leone TC, O'Donnell JM, Abel ED, Kelly DP, et al. Preferential oxidation of triacylglyceride-derived fatty acids in heart is augmented by the nuclear receptor PPARalpha. Circulation research. 2010;107:233-41.
[4] O'Donnell JM, Fields AD, Sorokina N, Lewandowski ED. The absence of endogenous lipid oxidation in early stage heart failure exposes limits in lipid storage and turnover. J Mol Cell Cardiol. 2008;44:315-22.
[5] Schaffer JE. Lipotoxicity: when tissues overeat. Current opinion in lipidology. 2003;14:281-7.
[6] Lehman JJ, Boudina S, Banke NH, Sambandam N, Han X, Young DM, et al. The transcriptional coactivator PGC-1alpha is essential for maximal and efficient cardiac mitochondrial fatty acid oxidation and lipid homeostasis. Am J Physiol Heart Circ Physiol. 2008;295:H185-96.
[7] Bowyer DE, King JP. Methods for the rapid separation and estimation of the major lipids of arteries and other tissues by thin-layer chromatography on small plates followed by microchemical assays. J Chromatogr. 1977;143:473-90.
[8] Williamson J, Corkey B. Assays of intermediates of the citric acid cycle and related compounds of fluorometric enzyme methods. New York, NY: Colowick SP
Kaplan NO; 1969.
[9] Yu X, White LT, Doumen C, Damico LA, LaNoue KF, Alpert NM, et al. Kinetic analysis of dynamic 13C NMR spectra: metabolic flux, regulation, and compartmentation in hearts. Biophys J. 1995;69:2090-102.
[10] Malloy CR, Sherry AD, Jeffrey FM. Evaluation of carbon flux and substrate selection through alternate pathways involving the citric acid cycle of the heart by 13C NMR spectroscopy. J Biol Chem. 1988;263:6964-71.
[11] Lewandowski ED, Doumen C, White LT, LaNoue KF, Damico LA, Yu X. Multiplet structure of 13C NMR signal from glutamate and direct detection of tricarboxylic acid (TCA) cycle intermediates. Magn Reson Med. 1996;35:149-54.
[12] Yu X, Alpert NM, Lewandowski ED. Modeling enrichment kinetics from dynamic 13C-NMR spectra: theoretical analysis and practical considerations. Am J Physiol. 1997;272:C2037-48.